2007

The Eirik Drift: a long-term barometer of North Atlantic deepwater flux south of Cape Farewell, Greenland

S. E. HUNTER, D. WILKINSON, J. STANFORD, D. A. V. STOW, S. BACON, A. M. AKHMETZHANOV & N. H. KENYON

National Oceanography Centre Southampton, University of Southampton Waterfront Campus, European Way, Southampton SO14 3ZH, UK (e-mail: sallyh@noc.soton.ac.uk)

Abstract: The Eirik Drift lies on the slope and rise off the southern tip of the Greenland margin where it formed under the influence of the North Atlantic deep western boundary current. The drift contains a semi-continuous and often expanded sedimentary record ranging from the Early Eocene to Holocene and so contains a record of bottom and intermediate current strengths over decadal to millennial time scales. These variations in current strength can be related to changes in thermohaline circulation and climate. The drift body is composed of four seismic sequences, with a number of internal discontinuities, reflecting a variety of palaeoceanographic events. Three secondary ridges are observed trending to the NW from the main ridge crest. The presence of these ridges, which have been active since the Early Pliocene, suggests that the deep current separates into three strands as it crosses the Eirik Drift, with each strand depositing a separate ridge. Variation in the degree of lateral migration within the Early to Late Pliocene sequence between ridges reflects local variation in the angle of slope on which the ridges formed. Cyclicity of reflector amplitude within the Late Pliocene to Pleistocene sequence could reflect changes in carbonate accumulation and deep current strength linked to glacial–interglacial variations.

The Eirik Drift is an elongate, mounded contourite drift lying on the slope and rise off the southern tip of the Greenland margin to the south of Cape Farewell (Fig. 1). The drift formed under the influence of the North Atlantic deep western boundary current (DWBC) mainly during the Pliocene and Pleistocene (e.g. Arthur *et al.* 1989). This current forms the main part of the deep, southward-flowing section of the North Atlantic thermohaline circulation system (THC). It is widely accepted that the shallow, northward-flowing limb of this circulation system is responsible for the relatively warm modern Northern European climate. THC is known to have varied on a number of time scales associated with different climatic events triggered by different forcings. On longer time scales, THC changes are thought to amplify the orbitally forced glacial–interglacial cycles. Increasing high-latitude sea-ice cover during cold periods can restrict deep-water formation, weakening or repositioning the THC. The resultant reduction in northward heat transport leads to regional cooling. This may in turn increase ice cover and planetary albedo, leading to global cooling. THC changes can also be triggered by more localized events such as the massive release of glacial meltwaters in areas of deep-water formation. Climate changes triggered by THC shifts can be exceptionally fast, typically less than 100 years. Examples of such 'rapid' climate changes include cooling events such as the Younger Dryas and 8.2 ka event (Broeker 2000; Clark *et al.* 2002; Rahmstorf 2002).

Q1, Q2

Contourite drifts contain millennial-scale records, but with a resolution high enough to resolve decadal-scale events. The Eirik Drift contains a semi-continuous sedimentary record ranging from the Early Eocene to Holocene and, as such, provides an excellent opportunity to study past changes in North Atlantic THC. A considerable volume of literature exists regarding various aspects of the evolution, sedimentology, biostratigraphy and isotope geochemistry of the drift (e.g. Chough & Hesse 1985; Arthur *et al.* 1989) including a number of significant contributions resulting from Ocean Drilling Program (ODP) Leg 105 to the Labrador Sea and Baffin Bay (Srivastava *et al.* 1989*a*). However, the majority of these are regional studies and few focus solely on the Eirik Drift. The first aim of this paper is to provide a review of the existing literature regarding the Eirik Drift, focusing on large-scale drift evolution and associated palaeoceanographic events. Following this, new seismic data are presented and correlated with the existing seismic database for the area. Finally, contour mapping of the major seismic stratigraphic sequences is used to identify morphological variations throughout the evolution of the drift. Analysis of the seismic character and morphological variations within the seismic sequences allows improved understanding of drift development

From: VIANA, A. R. & REBESCO, M. (eds) *Economic and Palaeoceanographic Significance of Contourite Deposits*. Geological Society, London, Special Publications, **276**, 245–263.
0305-8719/07/$15.00

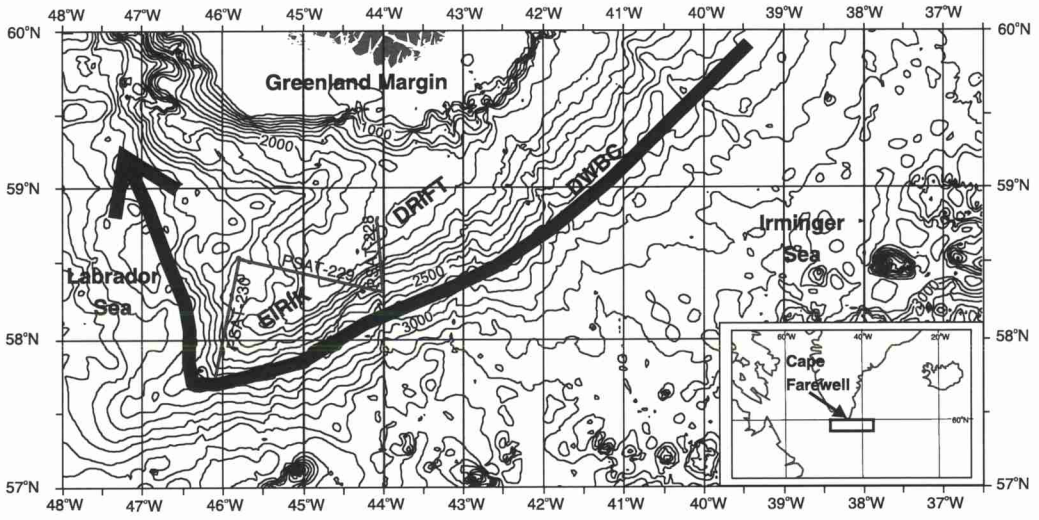

Fig. 1. Regional bathymetric map of the Eirik Drift area (Smith & Sandwell 1997). (See inset for location.) DWBC, Deep Western Boundary Current.

processes and the identification of long-term cycles of current variability within the Late Pliocene–Pleistocene sequence. This paper forms part of a continuing study of the sedimentary history of the Eirik Drift and the palaeoceanographic development in the Cape Farewell region, funded as part of the NERC Rapid Climate Change Program, which aims to provide a high-resolution, continuous, calibrated record of North Atlantic DWBC flux through the deglacial to Holocene period.

Tectonic setting

The Eirik Drift lies off the southern tip of Greenland at the junction between the Labrador Sea and the northern North Atlantic. The tectonic evolution of the area is therefore dominated by the opening history of these two basins. The formation of the Labrador Basin began with rifting between Greenland and Labrador during the Cenomanian (early Late Cretaceous) at the same time as sea-floor spreading was beginning in the North Atlantic. Rifting was followed by active sea-floor spreading in the southern Labrador Basin during the Campanian (mid-Late Cretaceous) and continued until the Late Eocene–Early Oligocene (Srivastava & Tapscott 1986).

The dominant structural trends in the study area relate to opening of the Labrador Basin and are composed of a series of NE–SW- and ENE–WSW-oriented fracture zones and associated perpendicular magnetic anomalies (Roest & Srivastava 1989). The Leif Fracture Zone, which lies just to the south of the Eirik Drift, separates older, continental–transitional crust of the southern Greenland margin to the NW from younger, deeply subsided oceanic crust to the SE, forming a relatively steep SE-facing slope (Arthur *et al.* 1989). An older fracture zone, the Farewell Fracture Zone, underlies the Eirik Drift and is associated with a WSW-trending basement high, which is thought to have controlled the initial formation of the drift (Le Pichon *et al.* 1971; Srivastava *et al.* 1987). A series of NW–SE-trending basement highs underlie the NW flank of the drift and run parallel to the magnetic anomalies in this area (Srivastava *et al.* 1987). Q3 Q3

Tectonics in the Norwegian–Greenland Sea region, particularly the subsidence history of the Greenland–Scotland Ridge, also exert a significant influence on the evolution of the Eirik Drift by forming a structural control on the flow of northern-sourced bottom waters into the North Atlantic. Rifting began in the Norwegian–Greenland Sea area during the mid-Late Cretaceous, but active sea-floor spreading did not begin here until the Early Eocene (Srivastava & Tapscott 1986). The Greenland–Scotland Ridge is a large regional swell in the oceanic crust between Greenland and Scotland associated with the mantle plume that currently underlies Iceland (Wright 1998). The subsidence history of the ridge has yet to be fully resolved but it has been established that the ridge had subsided sufficiently to allow the flow of northern-sourced bottom waters into the northern North Atlantic by the middle Miocene (Wright & Miller 1996; Wright 1998).

Oceanographic setting

The modern DWBC in the region of Cape Farewell is concentrated between the 1900 m and 3000 m isobaths towards the bottom of the continental slope (Clarke 1984). The DWBC transport is commonly accepted to be about 13–14 Sv (1 Sv = 1×10^6 m^3 s^{-1}); for example, Dickson & Brown (1994) quoted 13.3 Sv for the flow below the 27.80 isopycnal. Although this value is often referred to it is largely based on a single dataset collected in 1978 by the R. V. *Hudson* (Clarke 1984). Bacon (1998) calculated a much lower value of 6 Sv from data collected in 1991 by R. R. S. *Charles Darwin*, and Bacon (1998) argued that a comparison of data collected between 1958 and 1997 illustrates the decadal variability of the DWBC, which he attributed to changes in the output from the Nordic Seas.

The DWBC in the vicinity of Cape Farewell is composed of four main water masses (e.g. Dickson & Brown 1994): the Denmark Strait Overflow Water (DSOW), Iceland Scotland Overflow Water (ISOW), Labrador Sea Water (LSW) and modified Antarctic Bottom Water (AABW) (Fig. 2).

DSOW is composed of Nordic Sea intermediate waters that cross the Denmark Strait sill with a maximum depth of about 550 m. After crossing the sill the overflow waters descend rapidly, entraining ambient waters, primarily LSW. The resultant modified DSOW is identifiable as the lower layer of the DWBC off Cape Farewell. The transport of DSOW across the sill and into the DWBC is estimated to be 2.9 Sv (Dickson & Brown 1994; Fig. 2) increasing to around 10 Sv through entrainment on route to Cape Farewell.

Similarly, ISOW is composed of Nordic Sea intermediate waters that cross the Iceland Scotland Ridge to the east of Iceland. Dickson & Brown (1994) estimated the total eastern overflows to be about 2.7 Sv, of which 1.7 Sv flows through the Faeroe Bank Channel, where the maximum sill depth is about 850 m. The remainder overflows via a series of five smaller channels between Iceland and the Faeroes. The density of the ISOW is reduced by entrainment as it travels around the Reykjanes Ridge and into the Irminger Sea via the Charlie Gibbs Fracture Zone (CGFZ), such that it forms the upper layer of the DWBC at a depth of around 2000 m. The contribution of this modified ISOW to the DWBC off Cape Farewell is estimated at between 2 and 3 Sv (Dickson & Brown 1994; Schmitz 1996).

LSW is formed by wintertime deep convection in the Labrador and Irminger Seas. Originally, as the name suggests, it was thought to be formed solely in the Labrador Sea, but more recent work (Bacon *et al.* 2003; Pickart *et al.* 2003) has concluded that a second formation site exists in the Irminger Sea. LSW spreads across the North Atlantic and populates the low-velocity layer between about 700 m and 1500 m off the east coast of Greenland. LSW contributes a significant proportion of the DWBC as a result of entrainment with the two types of overflow water. Dickson & Brown (1994) estimated the contribution of LSW to the DWBC at around 4 Sv off Cape Farewell. However, inverse modelling has produced a value as high as 8 Sv (Alvarez *et al.* 2004).

AABW spreads north from its point of formation in the Antarctic and after modification joins the southward-flowing DWBC at various points in the North Atlantic. Estimates of the component joining off Greenland are in the region of 1–2 Sv (Schmitz & McCartney 1993; Schmitz 1996). A further 2 Sv is thought to be entrained, equally split between sites off Newfoundland and Florida.

In summary, the DWBC off Cape Farewell provides the major input to North Atlantic Deep Water (NADW). NADW is usually considered to have formed by the time the DWBC reaches the Grand Banks of Newfoundland (the deep water transported in the vicinity of Cape Farewell is therefore referred to as Proto North Atlantic Deep Water in Fig. 2) after further addition of LSW, AABW and ISOW in the Labrador Basin, although further modification does occur along its southward path. The transport of the DWBC is typically considered to be between 16 and 18 Sv as it flows across the equator and into the Southern Atlantic (Schmitz & McCartney 1993). As NADW is essentially the lower limb of the North Atlantic THC, the strength of the DWBC off Cape Farewell has a major influence on the THC. However, we still lack detailed knowledge about the drivers and variability of this current. This is an area of active research, and a series of moorings placed on the continental slope off Cape Farewell in summer 2005 as part of the NERC Rapid Climate Change Program is expected to provide valuable new data on the variability of the DWBC.

Database and methods

The seismic database used for this study consists of three new high-resolution, single-channel seismic lines along with a number of older, published single- and multi-channel sections (Arthur *et al.* 1989; Srivastava *et al.* 1989*b*; see Table 1). The new lines were acquired during the Training Through Research-13 (TTR-13) cruise to the northern North Atlantic onboard the R. V. *Professor Logachev* during July 2003 (Kenyon *et al.* 2004). Four seismic sequences (Seismic Sequences

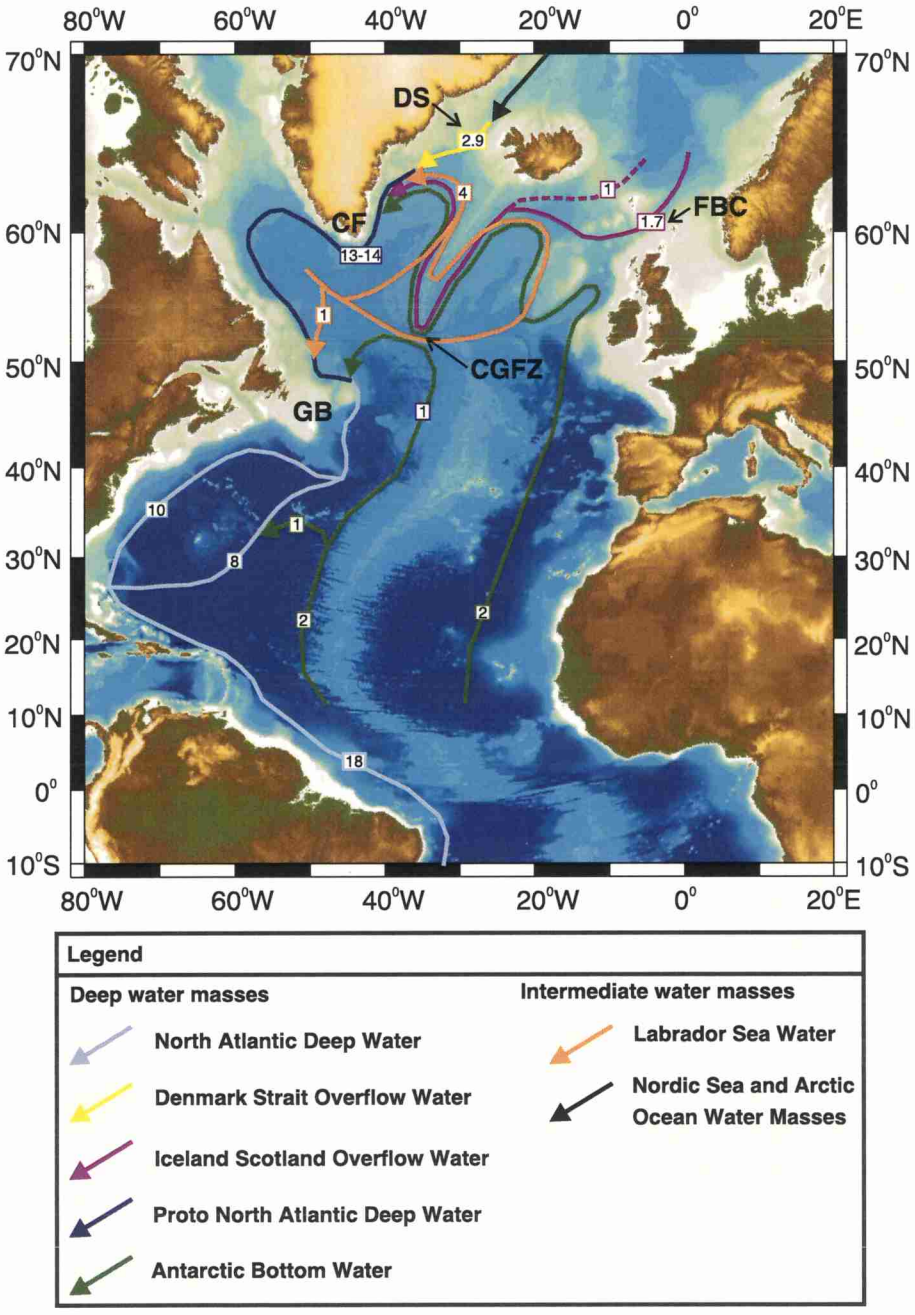

Fig. 2. Map of the North Atlantic region showing the water masses contributing to the formation of the North Atlantic Deep Water (modified from Schmitz 1996; Pickart *et al.* 2003). Boxed numbers refer to the volume flux in Sverdrups of the water masses at the locations indicated (see text for description). DS, Denmark Straits; CF, Cape Farewell; FBC, Faeroe Bank Channel; GB, Grand Banks; CGFZ, Charlie Gibbs Fracture Zone.

Color

Table 1. *Seismic sections used in this study*

Line number	Type	Cruise	Reference
PSAT-228	Single-channel	TTR-13	This study
PSAT-229	Single-channel	TTR-13	This study
PSAT-230	Single-channel	TTR-13	This study
Line 10	Single-channel	HU-84-30	Srivastava *et al.* 1989*b*
Line 11	Single-channel	HU-84-30	Srivastava *et al.* 1989*b*
Line 12	Single-channel	HU-84-30	Srivastava *et al.* 1989*b*
Line 14	Single-channel	HU-84-30	Srivastava *et al.* 1989*b*
Line 15	Single-channel	HU-84-30	Srivastava *et al.* 1989*b*
Line 16	Single-channel	HU-84-30	Srivastava *et al.* 1989*b*
Line 19	Single-channel	HU-84-30	Srivastava *et al.* 1989*b*
Line 20	Single-channel	HU-84-30	Srivastava *et al.* 1989*b*
Line 21	Single-channel	HU-84-30	Srivastava *et al.* 1989*b*
BGR-1	Multi-channel	BGR77	Arthur *et al.* 1989
BGR-2	Multi-channel	BGR77	Arthur *et al.* 1989

Q16

1, 2, 3 and 4) have been identified within the published sections (Arthur *et al.* 1989). These range in age from Early Eocene to Pleistocene and are described in following sections. Only the upper two of these sequences can be recognized in TTR-13 lines, because of their much shallower penetration.

Depths (in seconds two-way travel time (TWT)) to the base of the upper two seismic sequences have been mapped and contoured, along with the thickness (in seconds TWT) of Seismic Sequences 1 and 2 and the combined thickness of Seismic Sequences 3 and 4. A map of depth to basement has been constructed from a compilation of published maps (Srivastava *et al.* 1987; Le Pichon *et al.* 1971; Tucholke & Fry 1985) with additional data from the new and old seismic sections.

Q3

Bathymetry

A new bathymetric map of the Eirik Drift has been constructed, based on the seismic lines listed in Table 1 along with unpublished bathymetric data from a recent cruise to the area by the R. R. S. *Charles Darwin*, and merged with the bathymetry of Smith & Sandwell (1997) around the margins of the drift. The new bathymetric map, presented in Figure 3, shows a similar pattern to the regional bathymetry of Smith & Sandwell (1997; Fig. 1), but more clearly shows the presence of three NW-trending secondary ridges on the northern drift flank. The new map is significantly different from GEBCO bathymetric charts, with the major difference being that the current dataset shows no evidence of a secondary, SW-trending ridge to the north of the main ridge crest as shown in GEBCO charts.

The Eirik Drift has an elongated, mounded morphology with a length/width ratio of *c.* 2:1 and elongation direction to the SW, oblique to the southern Greenland margin from which the drift extends. The main drift crest descends from around 1500 m adjacent to the Greenland slope to 3500 m at 360 km to the SW. The southern flank of the drift, facing the SW-flowing limb of the DWBC, is characterized by a relatively steep and regular slope of around 1.3°. The northern drift flank and drift crest display marked changes in slope, with variation between 0.3 and 1.5°. These variations in slope define three secondary ridges, which extend to the NW from the main drift crest and have relatively steep southwestern flanks facing the DWBC as it flows NW into the Labrador Sea. The secondary ridge crests occur at 2000–2300 m, 2100–2600 m and 3200–3400 m, with the depth of each increasing to the NW, and are numbered Secondary Ridge (SR) 1, 2 and 3, respectively.

Seismic stratigraphy and phases of drift construction: syntheses of the ODP Site 646 results

Seismic sequences

Four seismic sequences have been identified in the Eirik Drift region (Arthur *et al.* 1989; Srivastava *et al.* 1989*b*). These sequences have been described in detail by Arthur *et al.* (1989), with reference to drilling results from ODP Site 646 on the northern flank of the Eirik Drift (location shown in Fig. 3). The following description therefore derives from Arthur *et al.* (1989) unless otherwise stated.

The oldest seismic sequence, Sequence 4, is Early Eocene to Late Miocene in age and is generally acoustically transparent. It overlies basement and is characterized by marked thickness variations

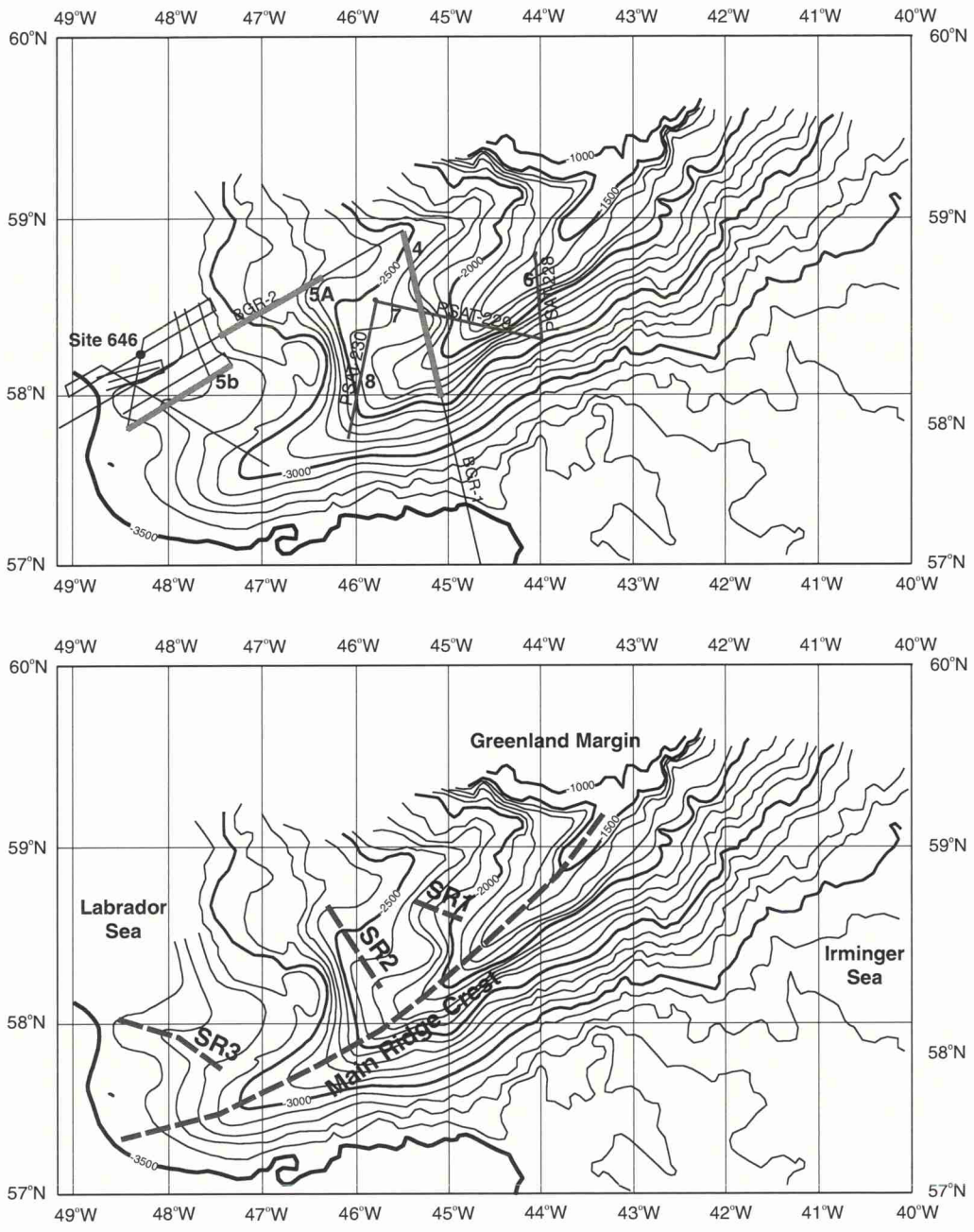

Fig. 3. New bathymetric map of the Eirik Ridge. The upper map shows the location of the seismic sections used in this study and the location of ODP Site 646. The positions of the main ridge crest and three secondary ridge crests are highlighted on the lower map.

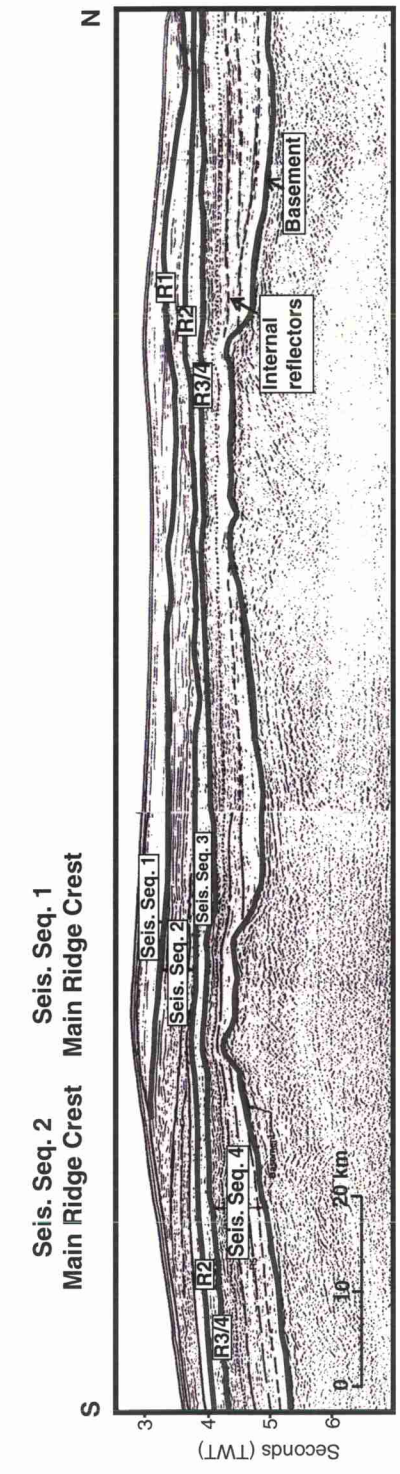

Fig. 4. Section from multi-channel line BGR-1 crossing the main ridge crest. From Arthur *et al.* (1989). (See location in Fig. 3.)

resulting from the infilling of irregular basement topography (Figs 4 and 5a and b). The overlying Sequence 3 is Late Miocene to Early Pliocene in age and consists of low- to moderate-amplitude reflectors forming a package of relatively uniform thickness throughout the area (Fig. 4). The upper part of Sequence 3 contains a prominent reflector (R2), which is dated at around 5.6 Ma, and thought to result from a short-term increase in carbonate preservation. Sequences 3 and 4 are separated by a high-amplitude double reflector (R3–R4) that represents changes in carbonate content and deposit physical properties relating to a short-term decrease in sedimentation rate.

Seismic Sequence 2 (of Early to Late Pliocene age) overlies Sequence 3 with an erosional unconformity across most of the area, which is dated at 4.5 Ma and marks the onset of strong bottom-current activity. The sequence is characterized by the presence of very high-amplitude, parallel to subparallel, northward-dipping reflectors that form four distinct and coeval depositional ridges. The ridges show northward progradation and approximately underlie the ridges seen in the modern bathymetry (Figs 4 and 5a and b). Migrating sediment waves are described within this sequence, although these are difficult to resolve within the published sections (Fig. 5b). Arthur *et al.* (1989) interpreted these characteristics as indicating that this sequence was deposited under the influence of significant bottom-current flow. A prominent reflector at 340 mbsf (metres below sea floor) at Site 646, dated at around 4 Ma, marks a change in the dominant biogenic material within the sediment from calcareous below to bio-siliceous above. This change reflects a significant cooling in surface waters at a time somewhat later than the onset of significant bottom-current activity. Also described at this time interval are erosional modification of the drift and changes in sediment grain-size and sorting parameters.

The uppermost seismic sequence, Sequence 1, is Late Pliocene to Pleistocene in age and consists of moderate- to high-amplitude reflectors that are parallel to subparallel to the sea floor and thought to be a function of local variations in the relative proportion of carbonate and clay in the sediment. The base of Sequence 1 is marked by a prominent reflector that coincides with the onset of ice-rafted sediment deposition in the area. Sequence 1 is generally conformable with Sequence 2, except in the vicinity of Sequence 2 ridge crests, where Sequence 1 onlaps the underlying unit (Fig. 4). Sequence 1 shows pronounced variations in thickness related to the upslope migration of ridge crests from Seismic Sequence 2 to 1. The characteristics of these sequences are summarized in Table 2.

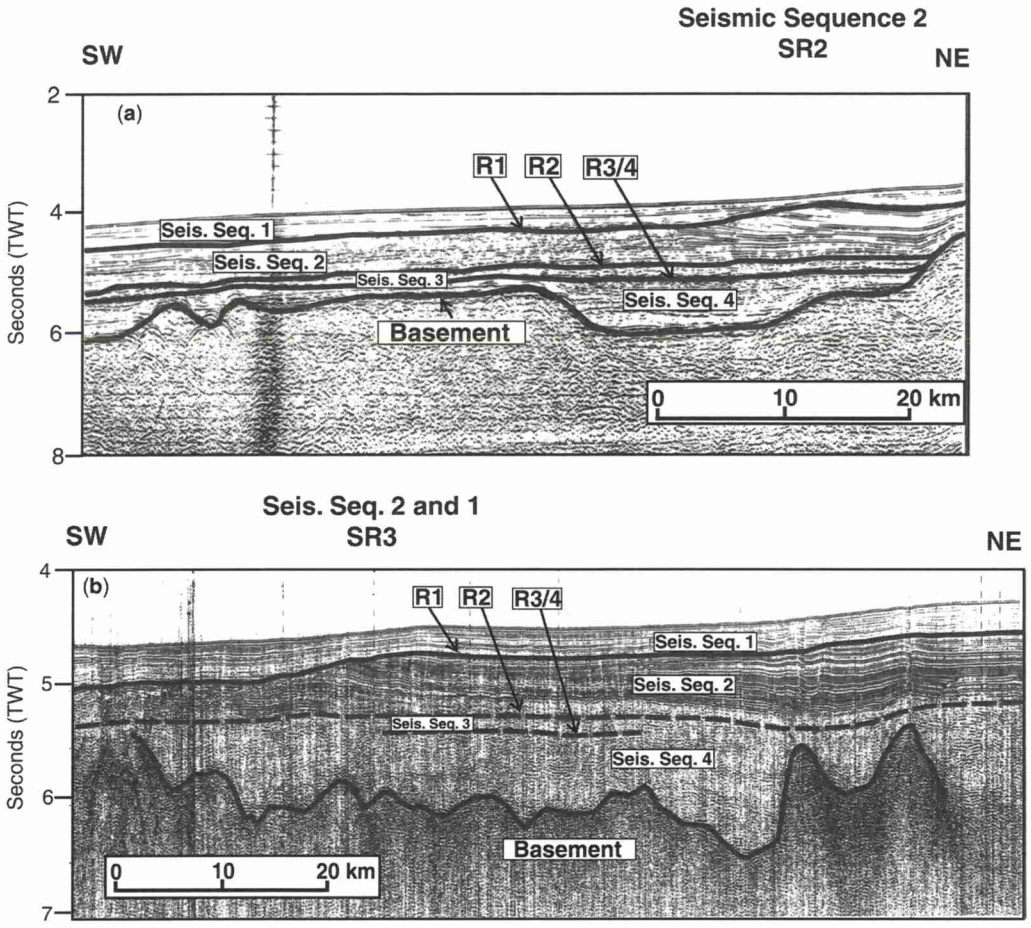

Fig. 5. (**a**) Section from multi-channel line BGR-2 crossing the central secondary ridge crest (SR2); (**b**) single-channel Line 15 crossing the southerly secondary ridge (SR3). From Arthur *et al.* (1989) and Srivastava *et al.* (1989*b*). (See locations in Fig. 3.)

Sedimentological, biostratigraphic and isotopic characteristics

Drilling results from ODP Site 646 show that all four seismic sequences are dominated by silty clays and clayey silts that are generally strongly bioturbated and contain variable proportions of biogenic material (Cremer *et al.* 1989), and are consistent with earlier core descriptions (Chough & Hesse 1985). Cremer *et al.* (1989) divided the sedimentary section of the Eirik Drift into two lithological sequences, with the upper lithological sequence corresponding to Seismic Sequence 1 and the lower sequence corresponding to Seismic Sequences 2, 3 and 4. These lithological sequences are distinguished on the basis of coarse sediment content, with the upper sequence showing a marked increase in the greater than 63 μm fraction. This coarse fraction in the upper lithological sequence contains some very large clasts and reflects the onset of ice rafting in the Eirik Drift area.

Variations in grain size within the lower lithological sequence were interpreted by Cremer (1989) as reflecting changes in bottom-current intensity during the Late Miocene and Early Pliocene. Cremer noted an increase in median grain size around the R3–R4 reflector (separating Seismic Sequences 3 and 4) resulting from increased bottom-current influence at around 7.5 Ma. This event is followed by generally decreasing grain size, indicating weakening bottom-current influence, until around the depth of the R2 reflector, when grain size increases again, marking increased

Table 2. *Principal characteristics of the seismic sequences in the Eirik Drift area summarized from Arthur et al. (1989) and Srivastava et al. (1989b)*

Principal characteristics
Seismic Sequence 1; Late Pliocene to Pleistocene
Moderate- to high-amplitude reflectors, parallel to subparallel to the sea floor
Base (reflector R1) is conformable to unconformable with Sequence 2 with onlap in some areas
R1 is a very high-amplitude reflector closely corresponding to the onset of ice rafting in the area
Thinnest over Sequence 2 ridge crests and thickest on the lee sides of Sequence 2 ridges
Seismic Sequence 2; Early to Late Pliocene
High-amplitude parallel to subparallel, commonly dipping reflectors
Sequence contains a number of pronounced depositional ridges
Migrating sediment waves common
Base conformable to unconformable with Sequence 3, with an erosional contact in some Areas
Seismic Sequence 3; Late Miocene to Early Pliocene
Continuous to discontinuous low- to moderate-amplitude reflectors
Contains a moderate- to high-amplitude reflector (R2) in upper part of sequence
Sequence has a generally constant thickness
Base marked by high-amplitude double reflector (R3–R4) and is conformable to unconformable with Sequence 4
Seismic Sequence 4; Early Eocene to Late Miocene
Generally acoustically transparent with the exception of a prominent reflector (R5) near the base of the sequence
The sequence overlies basement and shows pronounced thickness variations, thinning across basement highs and thickening into adjacent troughs

bottom-current activity at around 5.6 Ma. Silt beds first appear in the sequence at around the base of Seismic Sequence 2, indicating the onset of strong bottom-current activity (Cremer 1989) concurrently with the onset of drift construction observed in seismic sections (Arthur *et al.* 1989).

Study of the benthic Foraminifera revealed the occurrence of several distinct assemblages characterizing the different seismic sequences, with turnovers in assemblage reflecting changes in water-mass properties (Kaminski *et al.* 1989). The following description of benthic foraminiferal assemblages and associated palaeoenvironmental and palaeoceanographic interpretations is summarized from Kaminski *et al.* (1989).

Seismic Sequence 4 (Early Eocene to Late Miocene) is associated with a benthic foraminiferal assemblage dominated by *Nuttallides umbonifera*, with associated fine agglutinated species. This assemblage represents an environment with low current energy and corrosive bottom waters undersaturated with respect to calcium carbonate. In contrast, Seismic Sequence 3 (Late Miocene to Early Pliocene) is dominated by an assemblage of coarse agglutinated taxa with affinities to Norwegian–Greenland Sea faunas, with subordinate species associated with environments influenced by NADW-type water masses. This assemblage suggests an environment with significant northern-sourced bottom-current flow. This major change in benthic ecology between Seismic Sequences 4 and 3 was interpreted by Kaminski *et al.* (1989) as marking the onset of the flow of Denmark Straits Overflow Water (DSOW) into the Eirik Drift area.

Agglutinated taxa disappear before the deposition of Seismic Sequence 2 (Early to Late Pliocene), suggesting increasing current strength. Seismic Sequence 2 contains a high proportion of calcareous species typical of modern deep-water environments influenced by components of the NADW. This association therefore suggests increased strength of northern-sourced bottom-water currents. Seismic Sequence 1 (Late Pliocene to Pleistocene) contains low-abundance benthic associations typical of glacial environments, indicating the onset of glacial conditions.

Isotopic, planktonic formainiferal, sediment flux and magnetic grain-size studies of the Pleistocene part of the drift sequence reveal strong glacial–interglacial cyclicity. Deep-water areas show generally increased terrigenous and pelagic sediment accumulation rates during interglacial stages and low magnetic grain size and relatively low sediment accumulation rates during glacial stages (Hall *et al.* 1989; Hillaire-Marcel *et al.* 1994). Conversely, sediment accumulation rates at intermediate depths are higher during glacial stages, with relatively condensed interglacial sediments reflecting low sedimentation rates and/or erosion (Hillaire-Marcel *et al.* 1994).

New seismic sections

Seismic sequences and deposit geometry

The new seismic sections are of higher resolution than the published sections and cross both the main SW-trending ridge and the northern and

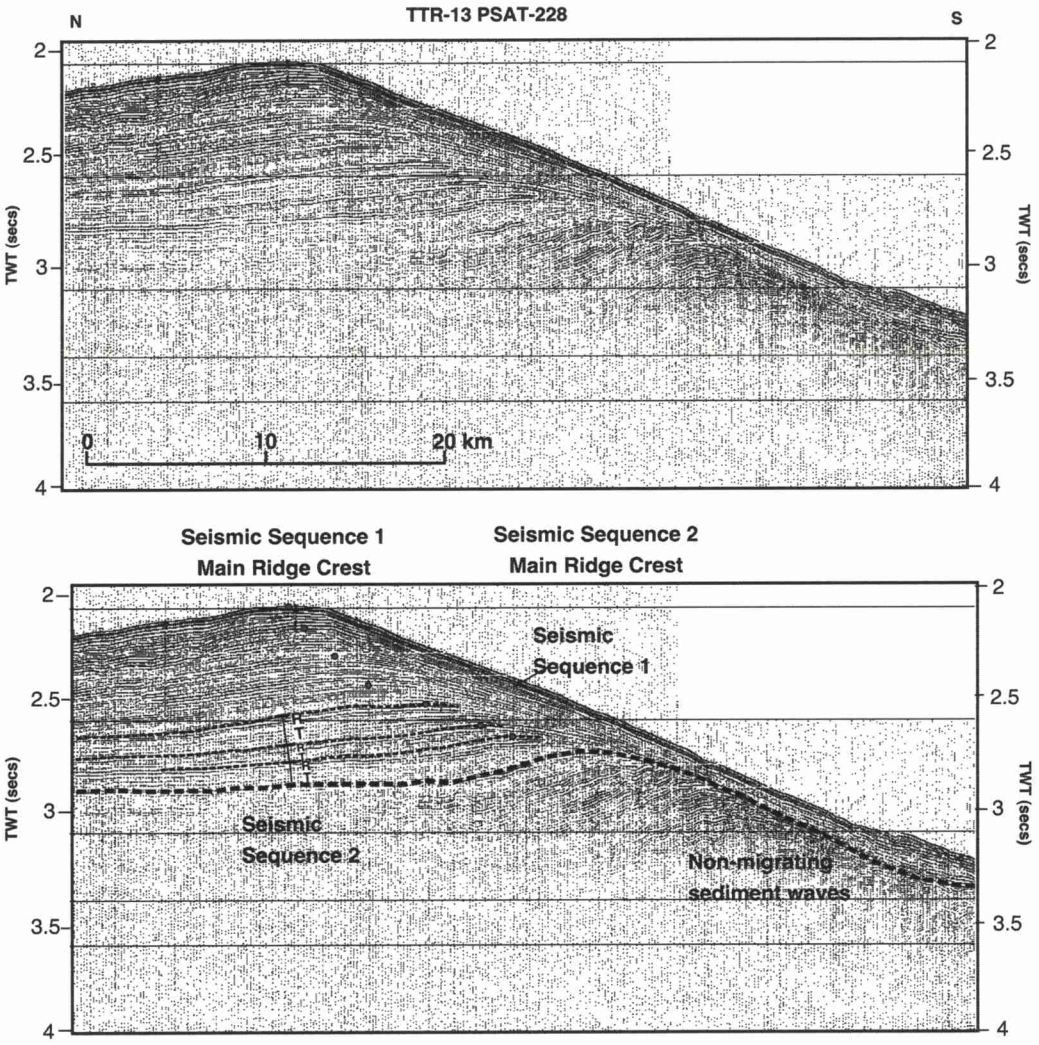

Fig. 6. Line PSAT-228 with uninterpreted section above and interpreted section below. (See Fig. 3 for location.) Within Seismic Sequence 1, T and R indicate alternating transparent and reflective seismic character, and the grey spots mark the position of successive ridge crests to highlight variations in lateral migration.

central secondary NW-trending ridges (locations shown in Fig. 3). PSAT-228 (Fig. 6) crosses the main ridge crest at the most northerly point of any of the seismic sections used in this study. PSAT-229 (Fig. 7) also crosses the main ridge, just to the south of PSAT-228, as well as the southern end of the most northerly secondary ridge (SR1). PSAT-230 (Fig. 8) does not cross the main SW-trending ridge crest, but instead crosses the central secondary ridge (SR2).

Two sequences can be recognized within these high-resolution seismic sections, with the upper and lower sequences correlating with Seismic Sequences 1 and 2 of Srivastava *et al.* (1989), respectively. The upper sequence can therefore be dated as Late Pliocene to Pleistocene in age and the lower sequence as Early to Late Pliocene. Q4

Seismic Sequence 2: Early to Late Pliocene. Sequence 2 displays the same general characteristics as described by Arthur *et al.* (1989) and Srivastava *et al.* (1989), with a series of high-amplitude reflectors forming pronounced depositional ridges. The new seismic sections allow more detailed observations of the internal structure within Sequence 2 ridge crests to be made.

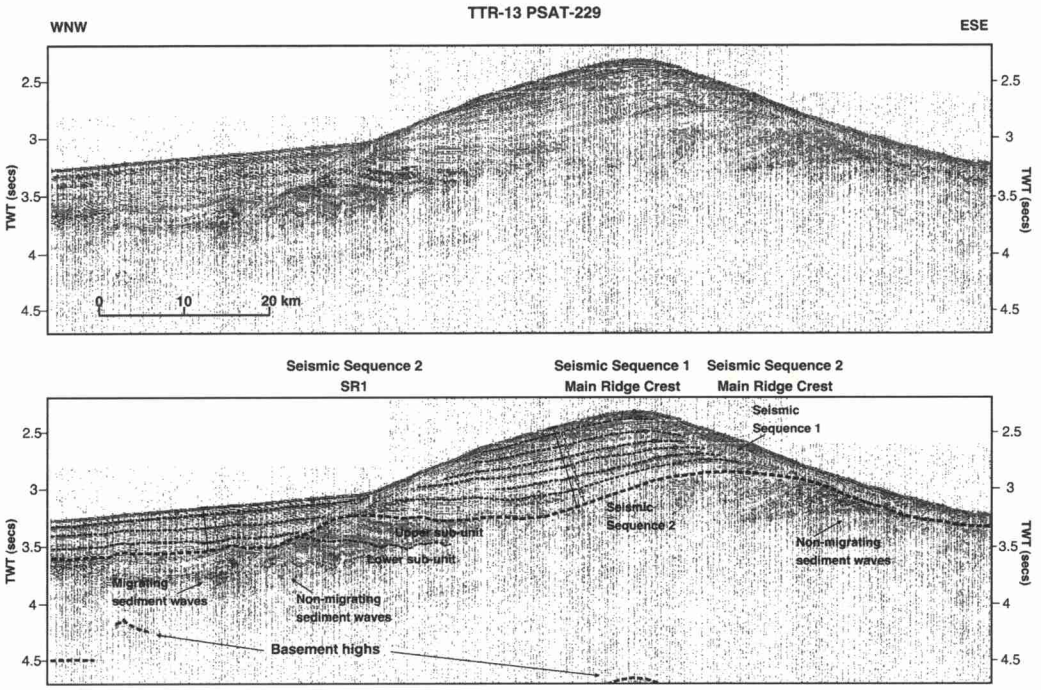

Fig. 7. Line PSAT-229 with uninterpreted section above and interpreted section below. (See Fig. 3 for location.) Within Seismic Sequence 1, T and R indicate alternating transparent and reflective seismic character, and the grey spots mark the position of successive ridge crests to highlight variations in lateral migration.

The main Sequence 2 ridge is composed of north-dipping reflectors that show erosional truncation on the southern, current-facing flank and form a single large drift body (Figs 6 and 7). The sequence here contains numerous sediment waves that appear to be non-migratory (Fig. 6). The degree of lateral migration of the main crest is difficult to determine because of the erosion on the southern flank, but appears to be low. The northern secondary ridge (SR1) has a similar internal structure with approximately SE-dipping reflectors and widespread sediment waves that again appear to be non-migratory. Just downslope of the southeastern flank of SR1, sediment waves are observed, which migrate toward the ridge (Fig. 7). SR1 is composed of two sub-units with the ridge crest stepping upslope, with *c.* 5 km of lateral, approximately westward migration between crests of successive sub-units (Fig. 7). The central secondary ridge crest (SR2) shows a different internal structure again (Fig. 8), being composed of several small, stacked build-ups with a total of 12 km of lateral upslope migration to the NW between successive crests, as previously described by Earley *et al.* (2002) from seismic sections just to the north of PSAT-230. Earley *et al.* (2002) interpreted this stacking pattern as reflecting shallowing of the core of the DWBC, with new build-ups forming upslope of the previous one as the current shallows.

Three very different internal ridge structures are therefore observed, with the main differences between types being the number of internal sub-units and degree of lateral migration between sub-units.

Seismic Sequence 1: Late Pliocene to Pleistocene. This sequence again shows the same general characteristics as described by Srivastava *et al.* (1989), but again the new seismic sections allow the recognition of more detailed features. The sequence is dominated by moderate- to high-amplitude reflectors, parallel to subparallel with the sea floor, forming sedimentary ridges upslope from the Sequence 2 ridges, as described by Srivastava *et al.* (1989). Marked variations in the degree of lateral migration of the drift crests are observed up-sequence, with rapid initial migration and minimal migration toward the top of the sequence (Figs 6–8). This pattern is observed on both the main drift crest and the central secondary ridge.

The new sections reveal cyclicity of reflector amplitude within this upper sequence, with each

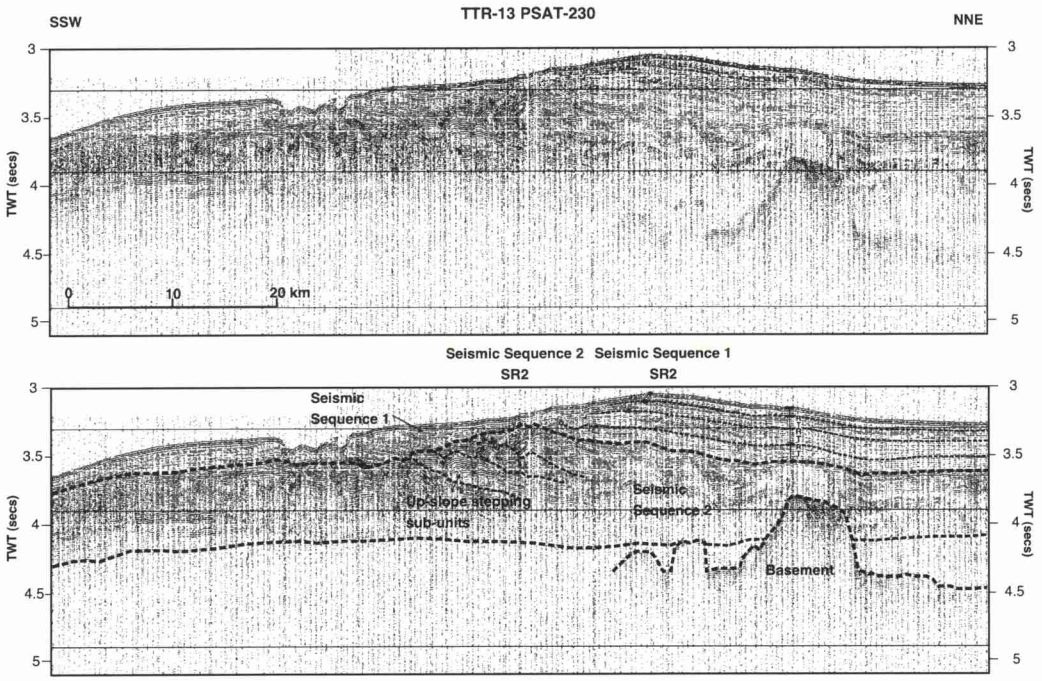

Fig. 8. Line PSAT-230 with uninterpreted section above and interpreted section below. (See Fig. 3 for location.) Within Seismic Sequence 1, T and R indicate alternating transparent and reflective seismic character, and the grey spots mark the position of successive ridge crests to highlight variations in lateral migration.

cycle consisting of a lower section of low- to moderate-amplitude reflectors (marked with a T in Figs 6–8 to denote relatively transparent seismic character) overlain by a high-amplitude section (marked with an R in Figs 6–8, indicating the more reflective seismic character). The number of visible cycles varies, with up to seven cycles being observed within the main Sequence 2 ridge crest (Fig. 7) and a minimum of four cycles observed in the central secondary ridge (Fig. 8). This pattern is similar to that described by Stow *et al.* (2002) from the Faro–Albuferia drift complex in the Gulf of Cadiz, which those researchers interpreted as representing changes in sand content and sedimentation rate linked to variations in bottom-current intensity. As reflectors in this upper sequence of the Eirik Drift are thought to result primarily from changing relative proportions in carbonate and clay (Arthur *et al.* 1989), this pattern of alternating amplitude is likely to reflect long-term changes in surface- and/or bottom-water conditions moderating this balance.

Seismic sequence morphology

Basement and Sequence 2 and 1 basal surfaces. Mapping depth to basement reveals a complex pattern of basement highs (Fig. 9a). On the NW flank of the drift, a series of NW–SE-trending highs occur that are parallel to the trend of magnetic anomalies in this area (Srivastava *et al.* 1987). To the east, the structural pattern becomes less clear. A number of seismic sections of various vintages cross this area (Le Pichon *et al.* 1971; Arthur *et al.* 1989), including the new TTR-13 lines. From these published sections, earlier workers have interpreted the presence of a NE–SW-trending basement high associated with the Farewell Fracture Zone underlying the main crest of the Eirik Drift (Le Pichon *et al.* 1971; Srivastava *et al.* 1987) This high plunges to the SW and is echoed in the plunge of the main drift crest. A number of lines also show basement highs to the north of this structure (e.g. the northern part of PSAT-230 (Fig. 8), the northern end of BGR-1 (Fig. 4) and the northern end of BGR-2 (Fig. 5a)), but the orientation of these structures is not fully resolved. These highs may form a series of approximately NE–SW-trending structures parallel to the Farewell Fracture Zone, although this study suggests that the highs observed on the eastern part of BGR-2 and northern part of PSAT-230 are connected, forming a NW–SE-trending high that is a continuation of the structural pattern

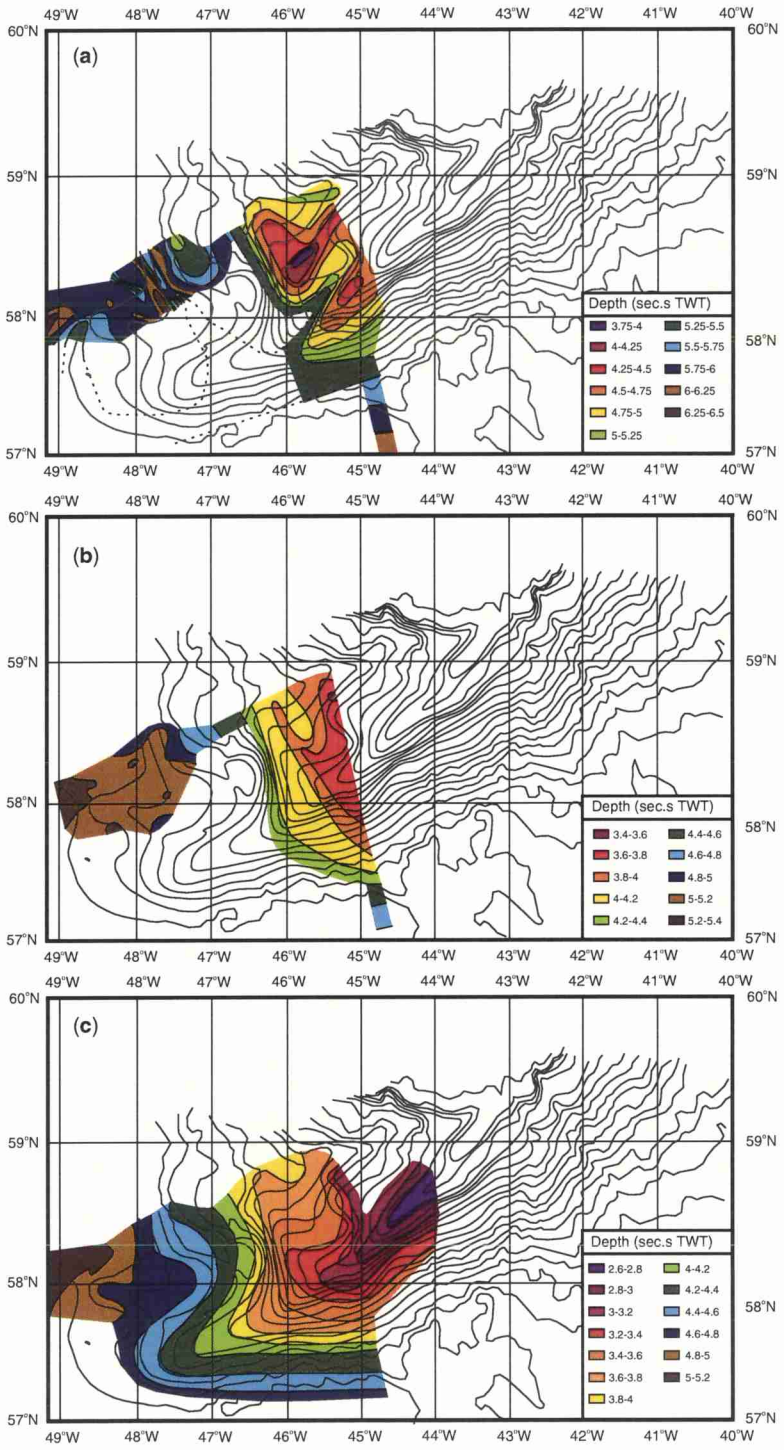

Fig. 9. Depth to basement and seismic sequence basal surfaces (seconds TWT). (**a**) Depth to basement (complied from Srivastava *et al.* 1987; 1989; and new data); (**b**) base Seismic Sequence 2; (**c**) base Seismic Sequence 1.

Q3, Q4

Color

observed in the west of the study area. Basement topography is very different on the southern flank of the Eirik Drift, with basement sloping steadily to the south.

The basal surface of Seismic Sequence 2 slopes relatively gently to the south and SW (Fig. 9b) but with significant local variations. To the south of the main ridge crest the base of Sequence 2 has a moderately steep and regular slope to the south, echoing that of basement. In the far west of the study area the base of Sequence 2 slopes very gently to the SW. The degree of slope increases to the east toward a relative high overlying the prominent basement structure observed at the northern ends of BGR-2 and PSAT-230. An approximately NW–SE-trending band of relatively steep slope overlies the southern flank of this basement high, with a depression in the base of Sequence 2 overlying the basement depression to the NW of the high. Between the relative high and the very gently sloping area in the west, the degree of slope varies from north to south, with a relatively steep and regular slope in the area of line BGR-2 and a much gentler slope to the south.

Depth to the base of Seismic Sequence 1 (Fig. 9c) shows a very similar pattern to the modern bathymetry, indicating that the structure of the drift was largely formed during the Early to Late Pliocene (Seismic Sequence 2) and has undergone only minor modifications during the Late Pliocene to Pleistocene.

Deposit distribution. The combined thickness of Seismic Sequences 3 and 4 shows trends similar to those of the map of depth to basement and displays thinning over basement highs and thickening into troughs (Fig. 10a). The limited expression of basement topography at the base of Seismic Sequence 2 shows that these units almost entirely fill in the basement topography. Several distinct thickness variations are visible within Seismic Sequence 2 (Fig. 10b), with the most prominent being the regions of increased thickness marking the main and secondary Sequence 2 ridges. A SW-trending area of increased thickness marks the main Sequence 2 ridge crest and is assumed to continue to the toe of the drift. Perpendicular to this, NW-trending zones in increased thickness mark the positions of SR1 and SR2. Between the intersections of these secondary ridges with the main ridge crest is an area of relatively reduced thickness. This relatively thin zone trends to the NW and overlies the basement high and relative high in the base of Seismic Sequence 2 in this area (described above). SR3 is marked by a zone of somewhat less pronounced thickening in the SW of the study area.

The map of Sequence 2 thickness also reveals a zone of thick Pliocene sediments forming a broad SW-trending tongue on the northern flank of the drift. This thick zone lies on trend with a major canyon in the SW Greenland margin and is likely to represent a sequence of Pliocene turbidites with sediments derived from this canyon.

Seismic Sequence 1 (Fig. 10c) shows distinct thinning over the relatively steep south- and SW-facing slopes of all the ridge crests, reflecting increased sediment winnowing or non-deposition resulting from significant, if intermittent, bottom-current activity along these slopes. This thin zone is wide over the southern side of the main ridge crest, reflecting a very thin sequence over the whole southern slope of the main Sequence 2 ridge. Thin zones are narrower and less pronounced overlying the SW-facing slopes of the secondary ridges, particularly SR3.

Sequence 1 is thickest upslope of the main Sequence 2 crest, with the zone of maximum thickness occurring on the main ridge crest to the north of the junction with SR1. Here the sequence reaches over 0.7 s TWT and appears to form one large accumulation upslope of both the main and northern secondary ridge crests (see Fig. 7). In contrast, only moderate thickening is observed upslope of SR2 and SR3. A broad area of thinner sediments is present overlying the zone of probable Pliocene turbidite deposition, suggesting a reduction in turbidite flow at this time.

Discussion

Drift construction and palaeoceanographic history

The history of drift construction and palaeoceanographic changes in the Eirik Drift area is summarized below and in Figure 11. The construction of the Eirik Drift began at 4.5 Ma, as shown by the pronounced sedimentary ridges developed within Seismic Sequence 2, and is thought to result from strong bottom-current activity in conjunction with high sediment input (Arthur *et al.* 1989). The main palaeoceanographic events preceding this phase of drift construction were the onset of the flow of DSOW at 7.5 Ma, following high-latitude cooling and subsidence on the Greenland–Scotland Ridge (Arthur *et al.* 1989; Wright 1998), and increasing bottom-current intensity at 5.6 Ma (Kaminski *et al.* 1989). At 4 Ma a change in the dominant biota reflects a cooling of surface waters (Arthur *et al.* 1989). Ice rafting began in the area at 2.5 Ma (Cremer *et al.* 1989) and was coincident with decrease in bottom-current intensity, upslope migration of drift crests and change in style of

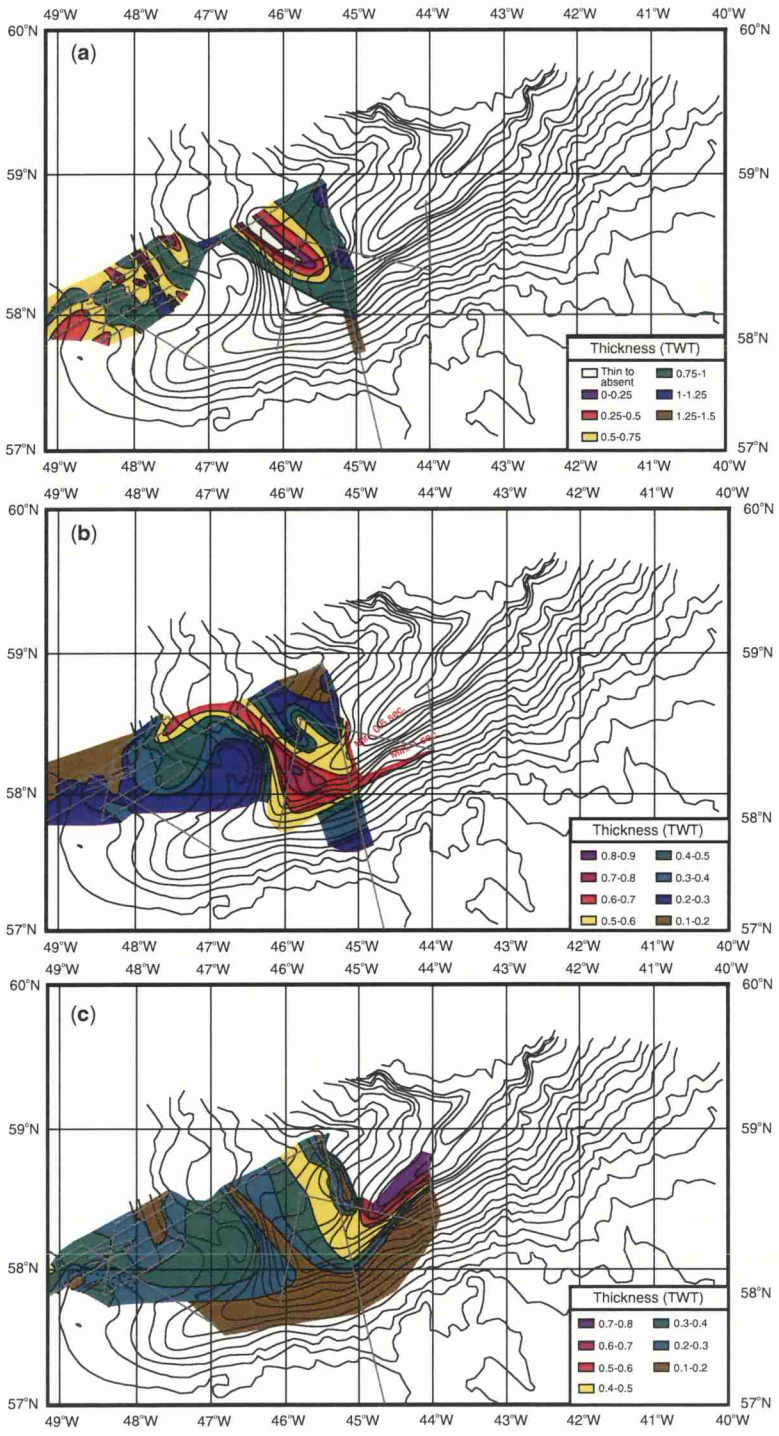

Fig. 10. Seismic sequence thickness distribution (seconds TWT). (**a**) Combined thickness of Seismic Sequences 3 and 4; (**b**) Seismic Sequence 2; (**c**) Seismic Sequence 1.

Color

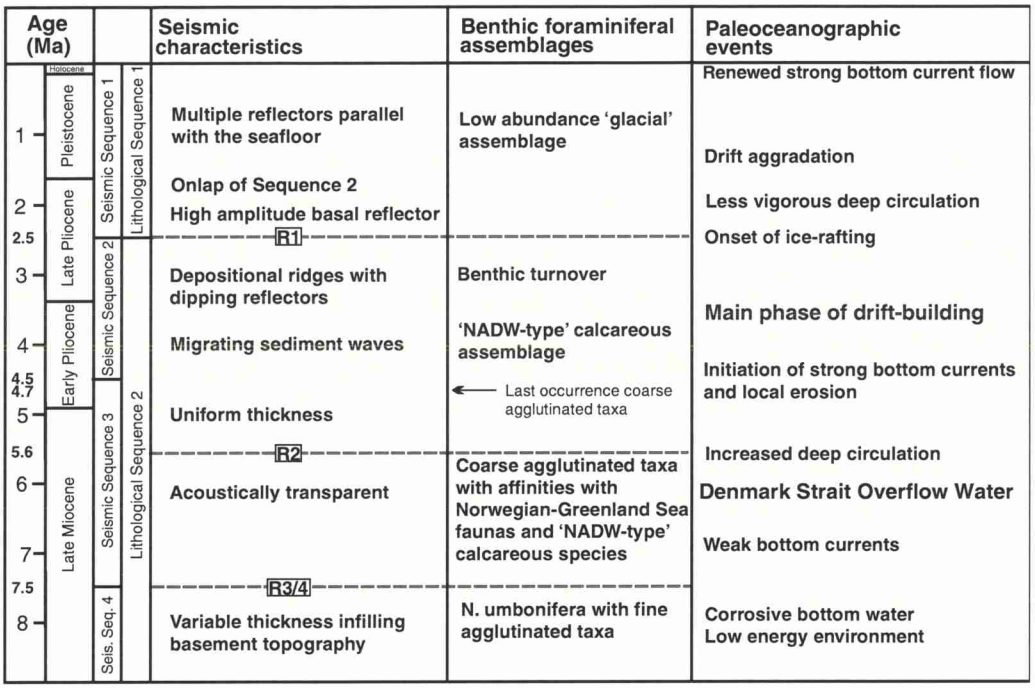

Fig. 11. Phases of drift construction and palaeoceanographic events in the Eirik Drift area. Modified from Arthur *et al.* (1989), Cremer *et al.* (1989) and Kaminski *et al.* (1989).

drift sedimentation (Arthur *et al.* 1989). These characteristics represent a major change in THC. Deep-water formation was restricted and intermittent during the Pleistocene, with the main southward-flowing current shifting to intermediate water depths (Glacial North Atlantic Intermediate Water; GNAIW). This shallowing and weakening of contour-current activity led to the observed upslope migration of ridge crests from Sequence 2 to Sequence 1 and the change in depositional style.

Glacial–interglacial cycles are recorded by isotopic, sedimentological and biological variations, with deep-water sites recording high sedimentation rates during interglacial periods when terrigenous and pelagic sediment fluxes were highest (Hall *et al.* 1989) and intermediate-level sites recording low sedimentation rates during interglacials as a result of increased current activity. The modern situation of renewed strong northern-sourced bottom-water flow was re-established during the Holocene (Hillaire-Marcel *et al.* 1994).

Early to Late Pliocene depositional architecture

Comparison of the internal structure of the different Early to Late Pliocene depositional ridges has revealed distinct variations in depositional architecture, with the main differences being the number of internal sub-units and the degree of lateral migration between sub-units. The central NW-trending ridge crest (SR2) contains the greatest number of sub-units and also displays the greatest degree of lateral migration between sub-units. Earley *et al.* (2002) suggested that these sub-units formed as a result of progressive shallowing of the core of the DWBC related to either warming or freshening of the current, an increase in current flux, which may raise the level of the current core in the water column, or an increase in the volume of AABW, which could displace the current upwards. All of these scenarios are plausible and detailed analysis of the Pliocene sedimentary section of the drift would be required to unequivocally determine the cause of current shallowing.

This pattern is not observed in any of the other ridge crests, or indeed at the northern end of SR2 (see line BGR-2, Fig. 5a), raising the question of why such oceanographic changes should be recorded by some ridges and not others. The most probable controlling factor is the initial degree of slope in the area of drift development. The southern end of SR2 formed over one of the most gently sloping areas of base Seismic Sequence 2

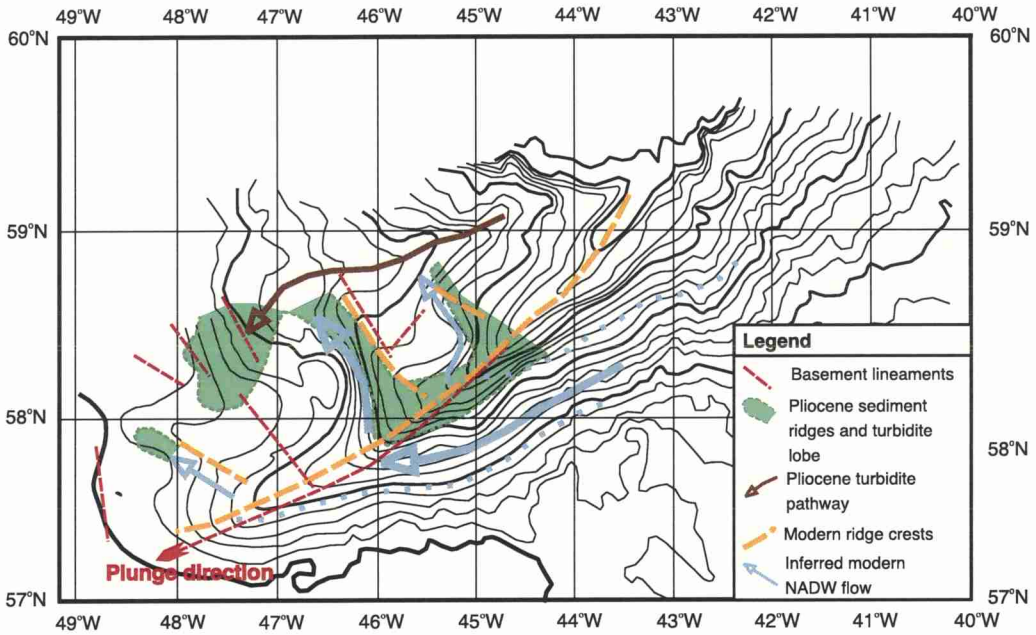

Fig. 12. Summary map showing basement structural trends, Pliocene and modern ridge crests, and the inferred path of Pliocene bottom currents.

Color

topography, which has presumably allowed the DBWC to migrate laterally more freely than in areas of steeper initial slope.

Pleistocene cycles

Analysis of the seismic character of Seismic Sequence 1 has revealed the presence of up to seven cycles of alternating low and high reflector amplitude. It is difficult to assess the exact frequency of these cycles. A maximum of seven cycles are observed within the main ridge crest, with a minimum of four cycles observed within SR1. This difference is presumably due to the expanded nature of the sequence on the main ridge crest with regard to SR1. This raises the possibility that more than seven cycles may exist, but that these could only be resolved by an even further expanded section. As reflectors in this sequence are thought to result from local variations in the proportion of carbonate and clay in the sediments (Arthur *et al.* 1989), and as interglacial periods are times of relatively high carbonate flux and increased winnowing (Hall *et al.* 1989; Hillaire-Marcel *et al.* 1994), it is suggested that these cycles reflect glacial–interglacial variations, with peak interglacial periods being represented by the reflective units in the upper part of each cycle.

Drift morphology; inferred DWBC pathways

This study has demonstrated that the Eirik Ridge is a complex body composed of four ridges that largely reflect Pliocene drift topography, with each ridge seen in the modern bathymetry being approximately underlain by a Pliocene counterpart (Fig. 12). The current system that deposited these Pliocene ridges is assumed to be broadly similar to the modern DWBC off Cape Farewell; that is, flowing south along the SW margin of Greenland before turning north around the distal end of the Eirik Drift and entering the Labrador Sea. The presence of the three NW-trending, coeval Pliocene depositional ridges branching to the NW from the main drift crest suggests that the Pliocene DWBC separated into three strands as it crossed the Eirik Drift, with each strand depositing a separate ridge. The cause of this flow separation appears to have been local variations in sea-bed topography at base Seismic Sequence 2 level, inherited from basement structure. The SW-flowing limb of the DWBC was confined along a relatively steep south-facing slope at base Sequence 2 level, leading to the deposition of the main Sequence 2 ridge crest as one large drift body. The additional SW direction of slope allowed the current to turn to the NW. It is suggested that instabilities within the flow, caused by local variations in the angle of this SW-dipping slope, led to flow separation, with

each separated strand depositing one of the secondary ridges. As the modern bathymetry still echoes Pliocene ridge structure, it seems likely that the modern DWBC also separates as it crosses the Eirik Drift.

Conclusion

Review of the existing literature allows the major palaeoceanographic events in the Eirik Drift area to be summarized. The relative timing of these events in the context of global and regional climatic changes has yet to be fully resolved; for example, the relative timing and significance of DWCB flux changes preceding Pliocene warming. More detailed analysis of the Neogene sedimentary section would provide valuable information to help resolve the issue of the relative timings of changes in THC and climatic events; that is, whether THC changes are a cause or consequence of documented climate changes (e.g. Kim & Crowley 2000).

Analysis of the seismic database in the area indicates the following features.

(1) Upslope stacking of multiple Pliocene drift crests reflects shallowing of the DWBC (Earley *et al.* 2002) but is recorded only within part of one ridge, indicating that variations in the degree of slope on which the drift builds form a limit on the degree of lateral migration of sedimentation for a given change in current depth.

(2) The Pleistocene sequence contains approximately seven cycles of reflector amplitude, which appear to be linked to glacial–interglacial variations in carbonate accumulation and deep current strength.

(3) Drift morphology suggests that the DWBC separates into three strands as it turns to the NW around the Eirik Drift and enters the Labrador Sea. It is suggested that this separation was caused by local variations in the degree of slope at base-drift level, causing funnelling of the current.

Continuing sedimentological and isotopic studies aim to unlock the decadal-scale records within the Eirik Drift sequence, so as to determine the sequence of variations in DWBC flux during the Holocene and deglacial period, and examine the relative timing and relationship of these changes in the context of short-term climatic events.

The authors would like to thank the Captain, officers and crew of the R.V. *Professor Logachev* and co-chief scientist M. Ivanov for the acquisition of the new seismic sections during the TTR-13 cruise, which was organized by the UNESCO–IOC Training Through Research Programme. Funding from the UK NERC Rapid Climate Change directed research programme (grant number NER/T/S/2002/00453) is gratefully acknowledged.

References

ALVAREZ, M., PEREZ, F. F., BRYDON, H. & RIOS, A. F. 2004. Physical and biogeochemical transports structure in the North Atlantic subpolar gyre. *Journal of Geophysical Research*, **109**, doi: C03027. Q5

ARTHUR, M., SRIVASTAVA, S. P., KAMINSKI, M., JARRARD, R. & OSLER, J. 1989. Seismic stratigraphy and history of deep circulation and sediment drift development in the Baffin Bay and the Labrador Sea. *In*: SRIVASTAVA, S. P., ARTHUR, M. & CLEMENT, B. (eds) *Proceedings of the Ocean Drilling Program, Scientific Results, 105.* Ocean Drilling Program, College Station, TX. Q6

BACON, S. 1997. Circulation and fluxes in the North Atlantic between Greenland and Ireland. *Journal of Physical Oceanography*, **27**, 1420–1435. Q7

BACON, S. 1998. Decadal variability of the outflow from the Nordic Seas to the deep Atlantic Ocean. *Nature*, **394**, 871–873.

BACON, S. 2002. The dense overflows from the Nordic Seas into the deep North Atlantic. *ICES Marine Science Symposia*, **215**, 148–155. Q8

BACON, S., GOULD, W. J. & JIA, Y. 2003. Open-ocean convection in the Irminger Sea. *Geophysical Research Letters*, **30**, 1246.

CHOUGH, S. K. & HESSE, R. 1985. Contourites from the Eirik Drift, south of Greenland. *Sedimentary Geology*, **41**, 185–189.

CLARK, P. U., PISIAS, N. G., SOTCKER, T. F. & WEAVER, A. J. 2002. The role of thermohaline circulation in abrupt climate change. *Nature*, **415**, 863–869.

CLARKE, R. A. 1984. *Transport through the Cape Farewell Flemish Cap section.* International Council for the Exploration of the Sea Report, **185**, 120–130.

CREMER, M. 1989. Texture and microstructure of Neogene–Quaternary sediments, ODP sites 645 and 646, Baffin Bay and Labrador Sea. *In*: SRIVASTAVA, S. P., ARTHUR, M. & CLEMENT, B. (eds) *Proceedings of the Ocean Drilling Program, Scientific Results, 105.* Ocean Drilling Program, College Station, TX. Q9

CREMER, M., MAILLET, N. & LATOUCHE, C. 1989. Analysis of sedimentary facies and clay mineralogy of the Neogene–Quaternary sediments in ODP site 646, Labrador Sea. *In*: SRIVASTAVA, S. P., ARTHUR, M. & CLEMENT, B. (eds) *Proceedings of the Ocean Drilling Program, Scientific Results, 105.* Ocean Drilling Program, College Station, TX. Q6

DICKSON, R. R. & BROWN, J. 1994. The production of North Atlantic Deep Water: sources, rates and pathways. *Journal of Geophysical Research*, **99**, 12319–12341.

EARLEY, R. J., MOUNTAIN, G. S., WRIGHT, J. D. & MANLEY, P. 2002. Bedform evolution on Eirik Drift: hi-res MCS evidence of North Atlantic Deep Water variability along the SW Greenland margin. *EOS Transactions, American Geophysical Union*, **84**(46), Fall Meeting Supplement, Abstract PP151C-0936. Q10

HALL, I. R., BLOEMENDAL, J., KING, J. W., ARTHUR, M. A. & AKSU, A. E. 1989. Middle to Late Quaternary sediment fluxes in the Labrador Sea, ODP leg 105, site 646: a synthesis of rock-magnetic, oxygen-isotopic, carbonate and planktonic foraminiferal data. *In*: SRIVASTAVA, S. P., ARTHUR, M. & CLEMENT, B. (eds) *Proceedings of the Ocean Drilling Program, Scientific Results, 105.* Ocean Drilling Program, College Station, TX.

HILLAIRE-MARCEL, C., DE VERNAL, A., BILODEAU, G. & WU, G. 1994. Isotope stratigraphy, sedimentation rates, deep circulation and carbonate events in the Labrador Sea during the last ~200 ka. *Canadian Journal of Earth Sciences*, **31**, 63–89.

KAMINSKI, M. A., GRADSTEIN, F. M., SCOTT, D. B. & MACKINNON, K. D. 1989. Neogene benthic foraminifera biostratigraphy and deep-water history of sites 645, 646 and 647, Baffin Bay and Labrador Sea. *In*: SRIVASTAVA, S. P., ARTHUR, M. & CLEMENT, B. (eds) *Proceedings of the Ocean Drilling Program, Scientific Results. 105.* Ocean Drilling Program, College Station, TX.

KENYON, N. H., IVANOV, M. K., AKHMETZHANOV, A. M., KOZLOVA, E. V. & MAZZINI, A. 2004. *Interdisciplinary studies of North Atlantic and Labrador Sea margin architecture and sedimentary processes.* IOC Technical Series, **68**.

KIM, S.-H. & CROWLEY, T. J. 2000. Increasing Pliocene North Atlantic Deep Water: cause or consequence of Pliocene warming? *Paleoceanography*, **15**(4), 451–455.

LE PICHON, X., HYNDMAN, R. D. & PAUTOT, G. 1971. Geophysical study of the opening of the Labrador Sea. *Journal of Geophysical Research*, **76**, 4725–4743.

PICKART, R. S., STRANEO, F. & MOORE, G. W. K. 2003. Is Labrador Sea Water formed in the Irminger Basin? *Deep-Sea Research I*, **50**, 23–52.

ROEST, W. R. & SRIVASTAVA, S. P. 1989. Sea-floor spreading in the Labrador Sea: a new reconstruction. *Geology*, **17**, 1000–1003.

RUDELS, B., FAHRBACH, E., MEINCKE, J., BUDEUS, G. & ERIKSSON, P. 2002. The East Greenland Current and its contribution to the Denmark Strait Overflow. *ICES Journal of Marine Science*, **59**, 1133–1154.

SCHMITZ, W. J., JR 1996. *On the World Ocean Circulation: Volume 1, Some Global Features/North Atlantic Circulation*. Woods Hole Oceanographic Institution, Woods Hole, MA.

SCHMITZ, W. J., JR & MCCARTNEY, M. S. 1993. On the North Atlantic circulation. *Reviews of Geophysics*, **31**, 29–49.

SMITH, W. H. F. & SANDWELL, D. T. 1997. Global sea floor topography from satellite altimetry and ship depth soundings. *Science*, **277**, 1956–1962.

SRIVASTAVA, S. P. & ARTHUR, M. 1989. Tectonic evolution of the Labrador Sea and Baffin Bay: constraints imposed by regional geophysics and drilling results from Leg 105. *In*: SRIVASTAVA, S. P., ARTHUR, M. & CLEMENT, B. (eds) *Proceedings of the Ocean Drilling Program, Scientific Results, 105.* Ocean Drilling Program, College Station, TX., 989–1009.

SRIVASTAVA, S. P. & TAPSCOTT, C. R. 1986. Plate kinematics of the North Atlantic. *In*: VOGT, P. R. & TUCHOLKE, B. E. (eds) *The Geology of North America, Volume M, The Western North Atlantic Region*. Geological Society of America, Boulder, CO, 379–404.

SRIVASTAVA, S. P., ARTHUR, M. & CLEMENT, B. (eds) 1989*a*. *Proceedings of the Ocean Drilling Program, Scientific Results, 105.* Ocean Drilling Program, College Station, TX.

SRIVASTAVA, S. P., LOUDEN, K. E., CHOUGH, S. K., *ET AL.* 1989*b*. Results of detailed geological and geophysical measurement at ODP Sites 645 in Baffin Bay and 646 and 647 in the Labrador Sea. *In*: SRIVASTAVA, S. P., ARTHUR, M. & CLEMENT, B. (eds) *Proceedings of the Ocean Drilling Program, Scientific Results, 105.* Ocean Drilling Program, College Station, TX, 891–919.

STOW, D. A. V., FAUGÈRES, J.-C., GONTHIER, E. G., *ET AL.* 2002. Faro–Albuferia drift complex, northern Gulf of Cadiz. *In*: STOW, D. A. V., PUDSEY, C. J., HOWE, J. A., FAUGÈRES, J.-C. & VIANA, A. (eds) *Deep-water Contourite Systems: Modern Drifts and Ancient Series, Seismic and Sedimentary Characteristics.* Geological Society, London, Memoirs, **22**, 137–154.

TUCHOLKE, B. E. & FRY, V. A. 1985. Basement structure and sediment distribution in the Northwest Atlantic Ocean. *AAPG Bulletin*, **69**, 2077–2097.

WRIGHT, J. D. 1998. Role of the Greenland–Scotland Ridge in Neogene climate changes. *In*: CROWLEY, T. J. & BURKE, K. (eds) *Tectonic Boundary Conditions for Climate Reconstructions*. Oxford University Press, Oxford, 192–211.

WRIGHT, J. D. & MILLER, K. G. 1996. Control of North Atlantic Deep Water circulation by the Greenland–Scotland Ridge. *Paleoceanography*, **11**, 157–170.